

On the nature of the black-body stars

Aldo Serenelli^{1,2}, René D. Rohrmann³, and Masataka Fukugita^{4,5}

¹ Institute of Space Sciences (ICE, CSIC) Campus UAB, Carrer de Can Magrans, s/n, E-08193, Barcelona, Spain
e-mail: aldos@ice.csic.es

² Institut d'Estudis Espacials de Catalunya (IEEC), C/Gran Capita, 2-4, E-08034, Barcelona, Spain

³ Instituto de Ciencias Astronómicas, de la Tierra y del Espacio (CONICET), Av. España 1512 (sur), 5400 San Juan, Argentina

⁴ Kavli Institute for the Physics and Mathematics of the Universe, University of Tokyo, Kashiwa 277-8583 Japan

⁵ Institute for Advanced Study, Princeton, 08540 NJ, USA

December 3, 2024

ABSTRACT

We study the physical nature of the black-body stars recently discovered. We use sets of white dwarf (WD) model atmospheres with pure-He, pure-H, and H/He mixtures to compute synthetic spectra and compare theoretical expectations with observations of the black-body stars. We find that the spectral properties of the black-body stars in the UV and the optical are reproduced to high-accuracy by helium dominated atmospheres possibly with trace amounts of hydrogen below the spectroscopic detection limit, $-8 \leq \log(N_{\text{H}}/N_{\text{He}}) \leq -6$, and typical $\log g = 8$ values corresponding to WDs of $0.6 M_{\odot}$. Pure-He models with $\log g = 8$ also provide a good match from 12000 down to $T_{\text{eff}} = 8500$ K, but fail to simultaneously fit the UV and optical colors for the cooler stars in the sample. However, pure-He models with $\log g = 9$ show a better match with the data, implying that black-body stars could be massive white dwarfs, around $\sim 1.2 M_{\odot}$. We find that the emerging spectrum has a Planck distribution shifted towards the blue compared to the expected shape based on the model effective temperature. The black-body temperatures determined from colors overestimate the actual T_{eff} of these stars by 400 K and up to 1000 K, depending on temperature and $\log(N_{\text{H}}/N_{\text{He}})$. We finally show that precision of end-of-mission Gaia parallaxes should allow disentangling whether the black-body stars have typical white dwarf masses or represent a massive, peculiar population.

Key words. white dwarfs — stars: atmospheres — stars: evolution — opacity

1. Introduction

Recently it has been uncovered (Suzuki & Fukugita 2017, hereafter SF17) that there are stars, albeit quite rare, that exhibit almost perfect black-body spectra with no apparent absorption lines. SF17 suggested that these black-body stars (BB-stars) are probably DB white dwarf stars with temperatures too low ($\sim 10^4$ K) to develop helium absorption features. However, it is not apparent whether these stars are really DB white dwarfs, while the distance and luminosity are consistent with this assignment. It is particularly unclear whether the continuum spectrum of DB white dwarfs can be so close to the black body spectrum.

In this work we study the nature of BB-stars by considering the spectral properties of white dwarf model atmospheres computed under different assumptions regarding their composition. We find that pure-He atmosphere models produce a black-body spectrum that matches observed BB-stars. Atmospheres dominated by helium, but containing trace amounts of hydrogen, can also reproduce the data. The effective temperature of the models that best fit BB-stars differs, however, from the estimated black-body temperature due to opacity effects. The difference between these temperatures depend on the black-body temperature as well as on the amount of hydrogen pollution of the atmosphere. Assuming that BB-stars are white dwarfs, we estimate their distances to be < 200 pc. The parallax fractional uncertainties based on Gaia's end-of-mission expectations range between 1 and 6%. Based on this, we expect it will be possible to determine the effective temperature of the BB-stars to a precision of 500 K. This will allow to test our models of He-envelope

white dwarfs. In this regard, BB-stars are not only excellent targets for calibration of photometric surveys, but they also open up the novel possibility of testing our understanding of cool, high-density stellar atmospheres.

In Section 2 we briefly review the model atmospheres used in this work. In Section 3 we show that models with pure-He composition or very low hydrogen pollution reproduce the black-body properties of BB-stars. In Section 4 we discuss the differences between the black-body (or color) and effective temperatures of models. Finally, in Section 6 we discuss the future possibility that with Gaia parallaxes the absolute fluxes could be used to test model atmospheres.

2. WD atmosphere models

The white dwarf model atmospheres used in this work have been computed within the assumption of plane-parallel geometry, LTE, radiative-convective and hydrostatic equilibrium. Convective energy transport is treated in the mixing-length (ML2) approximation. Particle populations for a mixture of hydrogen and helium (H , H_2 , H^+ , H^- , H_2^+ , H_3^+ , He , He^- , He^+ , He^{++} , He_2^+ , HeH^+ , and e^-) are derived from the occupation probability formalism. All relevant radiative opacities are considered. Details of the code can be found in Rohrmann et al. (2012) and references therein. We use two classes of models according to composition: pure-He, and He-dominated atmospheres with a H abundances $\log(N_{\text{H}}/N_{\text{He}}) = -2, \dots, -8.5$. Results for pure hydrogen atmospheres are also considered but only for reference.

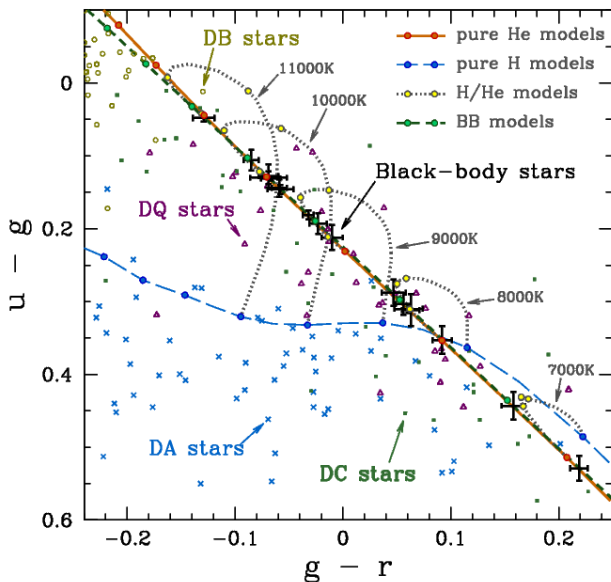


Fig. 1. Color-color diagram for a sample of white dwarf stars from the SDSS DR7 catalog (Kleinman et al. 2013). Black-body stars from SF17 are shown with error bars. Lines denote theoretical color-color curves for black-body (green short-dashed), pure-He (red/orange solid), pure-H (blue long-dashed), and mixed H/He (dotted) atmosphere models as indicated in the figure legend, in the range 12000–7000 K. Small circles on top of the curves showing black-body, He atmosphere and H atmosphere models indicate 1000 K intervals. Those on the bridging between H and He models mark the $\log(N_{\text{H}}/N_{\text{He}}) = -2, -4, -6$ values.

3. Black-body stars in the color-color plane

We present in Figure 1 the $(u - g)$ vs $(g - r)$ color-color diagram for white dwarfs from the SDSS DR7 white dwarfs catalog (Kleinman et al. 2013), where u, g, r are the SDSS color bands (Fukugita et al. 1996). We include DA (Balmer lines, no spectral features of other elements), DB (He 1 4471 Å), DC (featureless spectrum), and DQ (C2 Swan band or atomic CI lines) stars, where the spectroscopic classification is that from the original catalog. Randomly selected samples are shown for each class to avoid overcrowding the plot. The 17 BB-stars reported in SF17 are shown as black data points with error bars. The figure shows that the BB-stars might be identified as DQs or DCs, as both classes scatter around the location of the BB-stars. Both DQs and DCs are possible descendants of DBs.

Figure 1 includes theoretical predictions for different classes of white dwarf atmosphere models characterized by their composition. The orange solid line represents the predictions of pure-He atmosphere models for varying T_{eff} from about 13000 K (upper left) down to 7000 K (lower right). These models correspond to $\log g = 8$: $(u - g)$ and $(g - r)$ colors from pure-He atmospheres depend very weakly on $\log g$. The green short-dashed line represents results for black-body spectra. Circle ticks represent temperature intervals of 1000 K. The pure-He and the black-body curves overlap almost completely over the black-body temperature range between 11000 K and 7000 K. All BB-stars from SF17 fall in this temperature range and therefore lie perfectly on top of the pure-He models. We also note that at temperatures higher than approximately 11000 K the pure-He models start to deviate from the black-body curve. No BB-stars have been found at higher temperatures nor below 7000 K, a value below which pure-He models also start showing deviations from a black-body. We note, however, that this is by the selection of the sample of

SF17 that the spectrum should be close to the black-body. The star with a spectrum that deviated substantially from a black-body has been discarded. We note that not all DBs have spectra particularly close to a black-body as seen in the upper right corner of Figure 1.

Pure-H atmospheres have colors very different from a black-body spectrum in the temperature range of interest. These models are shown with blue long-dashed lines in Fig. 1. Colors of atmospheres composed of H/He mixtures vary with the relative abundance of H with respect to He. The dotted lines in the figure denote sequences of models with constant T_{eff} and decreasing amount of hydrogen going from the DA to the DB models. Here, yellow circle ticks denote $\log(N_{\text{H}}/N_{\text{He}}) = -2, -4$, and -6 . When the H/He ratio decreases to $\log(N_{\text{H}}/N_{\text{He}}) \lesssim -6$, they approach close to the pure-He models, within the observational uncertainties of BB-stars photometry. SF17 selected the BB-stars based on the absence of spectral features. It is to be noted that for $\log(N_{\text{H}}/N_{\text{He}}) \lesssim -6$ hydrogen lines remain hidden in helium-rich atmospheres; the equivalent width of H α drops below ~ 0.2 Å (Weidemann & Koester 1995).

It is also possible that the BB-stars are DQ stars with very small traces of carbon. Koester & Knist (2006) have shown that in C/He atmospheres the effect of carbon in the $(u - g)$ vs $(g - r)$ plane vanishes for $\log(N_{\text{C}}/N_{\text{He}}) < -8$ in the temperature range of the BB-stars. Spectroscopically, the lowest carbon abundance measured in DQ stars is $\log(N_{\text{C}}/N_{\text{He}}) \approx -7.5$ (Koester & Knist 2006; Kepler et al. 2015). On the other hand, evolutionary models (Camisassa et al. 2017) indicate that stars with pure-He envelope undergo a rapid enrichment of carbon due to dredge up. This evolution occurs as stars cool down from $T_{\text{eff}} \approx 12500$ K to 7000 K. The carbon abundance then increases up to $\log(N_{\text{C}}/N_{\text{He}}) \approx -3$ for white dwarf models of different stellar mass. Therefore, it does not seem plausible that the BB-stars, which are found across the same temperature range during which DBs are transformed into DQs, can have very low carbon abundances, right below the spectroscopic detection limit. This would require a very fine tuning between the efficiency of dredge up and gravitational settling.

We use Galex FUV and NUV data to study further the nature of the BB-stars. Figure 2 compares BB-stars with our models in the (FUV-NUV) vs $(g - r)$ plane. All BB-stars are perfectly matched by black-body colors. Pure-He models also provide a good description of the data for stars bluer than $(g - r) = 0.1$. For cooler stars with $(g - r) > 0.1$, the $\log g = 8$ canonical pure-He model deviates from the black-body results, and in particular does not reproduce the results for the three coolest BB-stars. Pure-He models show a larger sensitivity for the UV colors, and models with $\log g = 9$ remain close to black-body colors at cooler temperatures. This would suggest that the cool BB-stars could be quite massive white dwarfs with masses around $1.2 M_{\odot}$, i.e. in the realm of WDs with ONe or CO-Ne hybrid cores rather than typical CO cores (Althaus et al. 2005; Doherty et al. 2017). Less extreme results are found with the H/He models also shown in Figure 2 for $\log(N_{\text{H}}/N_{\text{He}}) = -5.4, -6$. These models at $\log g = 8$ reproduce the BB-stars better than pure-He models across the whole diagram, corresponding to typical WD masses of about $0.6 M_{\odot}$ in agreement with the mean mass value for DBs found by Koester & Kepler (2015).

Note that the temperature for the BB-stars may be somewhat lower, by the order of $100E(B - V)/0.01$ K, when extinction to these local white dwarfs is taken into account (SF17). It is difficult to determine extinction from photometry, since extinction is nearly parallel to the change of temperature.

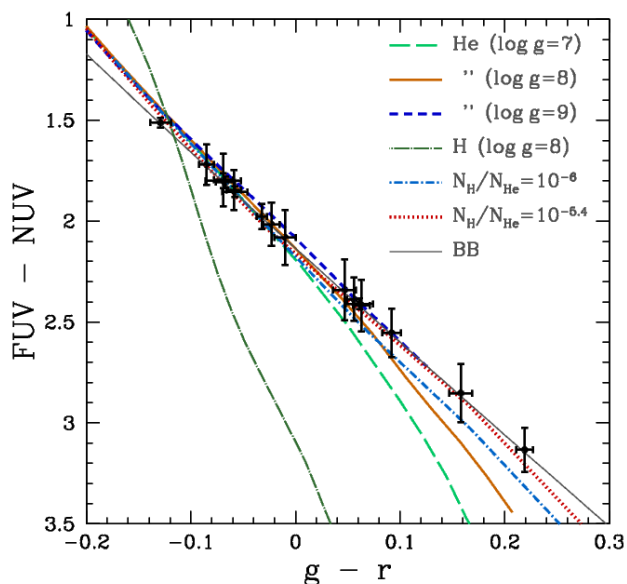


Fig. 2. (FUV-NUV)-(g-r) color-color diagram. BB-stars are shown as black dots with error bars. Lines denote theoretical models as indicated in the legend. Models with H/He mixtures correspond to $\log g = 8$. The H/He models with $\log(N_{\text{H}}/N_{\text{He}}) = -6$ reproduce all BB-stars data.

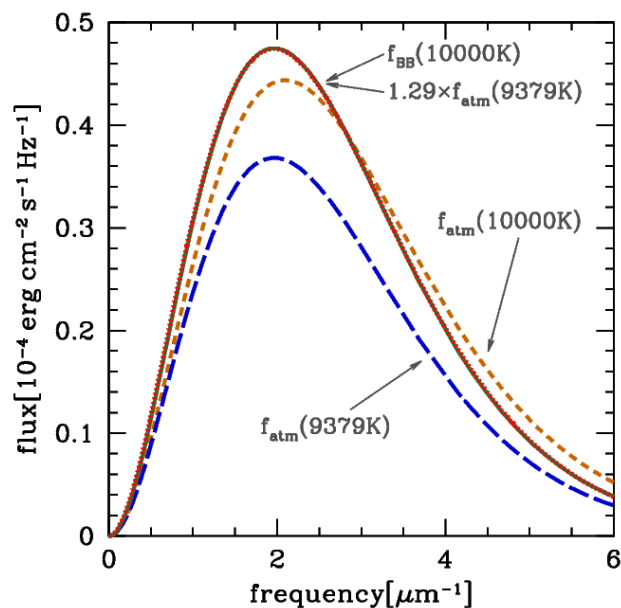


Fig. 3. Emerging monochromatic flux. Orange short dashed line: pure-He atmosphere with $T_{\text{eff}} = 10000$ K; solid green line: black-body spectrum with $T_{\text{eff}} = 10000$ K; blue long dashed line: pure-He atmosphere with $T_{\text{eff}} = 9379$ K; red dotted line: pure-He atmosphere with $T_{\text{eff}} = 9379$ K scaled up by a factor 1.29 to match the total flux of a $T_{\text{eff}} = 10000$ K spectrum. Model atmospheres correspond to $\log g = 8$.

4. BB-stars: color vs effective temperature

From the discussion above we find that BB-stars are most probably white dwarfs with mixed H/He envelopes with $-8 \leq \log(N_{\text{H}}/N_{\text{He}}) \leq -6$. Alternatively they could be massive white dwarfs with pure-He envelopes. In both cases, the properties of their atmospheres are determined to a large extent by their helium content. Based on this, we now look into the interpretation of the observed colors as temperature indicators of the BB-stars.

In Figure 3 we compare the emerging flux of a $T_{\text{eff}} = 10000$ K ($\log g = 8$) pure-He atmosphere with a black-body spectrum also at $T_{\text{eff}} = 10000$ K. The integrated flux in both models is the same and determined by the Stefan-Boltzmann law, $f(T_{\text{eff}}) = \sigma T_{\text{eff}}^4$, where σ is the Stefan-Boltzmann constant. The spectrum of the pure-He model is slightly shifted towards the bluer side, compared to the black body spectrum of the same T_{eff} . The figure also shows the spectrum of a pure-He model at $T_{\text{eff}} = 9379$ K, which reproduces the $T_{\text{eff}} = 10000$ K black-body spectrum, hence the colors, except for the flux normalization. This model has an integrated flux that is $(9379/10000)^4 = 0.774$ times the flux of the $T_{\text{eff}} = 10000$ K models. Similarly, the shape of the emerging spectrum of pure-He atmospheres is very close to a Planck function from about $T_{\text{eff}} = 12000$ K down to 8000 K or lower (for higher $\log g$ values) but corresponding to a different higher black-body temperature T_{BB} with $T_{\text{BB}} - T_{\text{eff}} = 500$ -800 K for $\log g = 8$. This is discussed in more detail later in this section.

The bluewards shift of spectrum of pure-He models with respect to a black-body of the same T_{eff} can be understood by looking at Figure 4, which shows the different contributions to the opacity of the model with $T_{\text{eff}} = 9379$ K at optical depth $\tau_{\text{Ross}} = 1$. Opacity is dominated by free-free (ff) He^- processes with ff and bound-free (bf) processes of He_2^+ as the secondary processes. These opacity sources have a relatively weak dependence with frequency across most of the spectrum but the dominant ff He^- contribution increases towards longer wavelengths (see Fig. 3). Increased flux blocking at longer wavelengths shifts the spectrum towards the blue, giving it the shape of a black-body of higher temperature but the same integrated flux. In the model shown in Fig. 3, bf transitions in He_2^+ become the single most important opacity source for frequencies larger than $5 \mu\text{m}^{-1}$, and increase for higher frequencies. Therefore, it is expected that colors involving UV bands will show deviations from black-body atmospheres when bf He_2^+ processes become dominant. Higher densities lead to a larger He_2^+ abundance and opacity but, because He_2^+ is the main donor of free electrons that form He^- , leads to an even higher ff He^- opacity, closer to grey opacity. This is particularly relevant to understand the impact of gravity on the spectral properties of He-dominated atmospheres and it is the main reason behind results in Figure 2 that show that for cool temperatures higher $\log g$ models remain closer to black-body than lower $\log g$ models.

The black-body, or color, temperature T_{BB} of our white dwarf model atmospheres differs from the effective temperature, as shown in Fig. 3 for pure-He models. The difference $T_{\text{BB}} - T_{\text{eff}}$ is shown in the bottom panel of Figure 5 as a function of T_{BB} for pure-He and H/He mixed atmosphere models. At $T_{\text{BB}} = 12000$ K the difference for the pure-He model is about 800 K, T_{BB} being higher, and it decreases steadily with decreasing T_{BB} to about 520 K at $T_{\text{BB}} = 7400$ K. Note that, although the shape of the spectrum in the model atmospheres resembles that of a black-body of temperature T_{BB} , the integrated flux is always given by σT_{eff}^4 . The figure also shows temperature corrections for H/He atmospheres with $\log(N_{\text{H}}/N_{\text{He}}) \leq -6$, below the current H abundance detection limit. There is a strong dependence of the temperature correction with the amount of H present in the atmosphere with the general trend that the difference increases for increasing H abundance. The reason for this behavior is that the presence of H leads to larger number of free electrons that enhance the contribution of the ff He^- opacity, the main driver of the spectral blue-wards shift.

The top three panels of Fig. 5 show the color differences between a black-body and the model atmospheres with different $\log(N_{\text{H}}/N_{\text{He}})$ values. Results for pure-He models are shown in

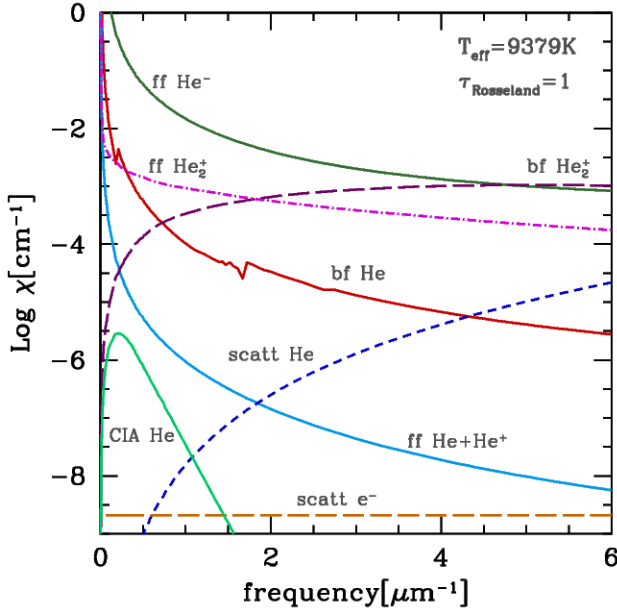


Fig. 4. Individual opacity contributions at $\tau_{\text{Ross}} = 1$ in a cool pure-He white dwarf atmosphere. Dominant contributions are ff processes of He^- and He_2^+ and bf processes of He_2^+ . Note that ff contribution from He^- increases markedly at low frequencies and is responsible for shifting the emerging spectrum towards higher frequencies making it appear hotter, i.e. $T_{\text{BB}} > T_{\text{eff}}$.

red dotted lines, for models with $\log(N_{\text{H}}/N_{\text{He}}) = -6$ in solid blue lines and for the best-fit models with varying $\log(N_{\text{H}}/N_{\text{He}})$ in dashed orange. Differences are shown as a function of the inferred T_{BB} (color temperature) value. Circles denote residuals results of the best black-body fit to the 17 BB-stars. The $\log(N_{\text{H}}/N_{\text{He}})$ values of the best fit models are shown in the fourth panel, where the level $\log(N_{\text{H}}/N_{\text{He}}) = -6$ is given for reference. Here we note that the best-fit models have in most cases $\log(N_{\text{H}}/N_{\text{He}}) = -5.4$, somewhat above our adopted formal spectroscopic detection limit. However, it is apparent that the models with lower $\log(N_{\text{H}}/N_{\text{He}})$ values also reproduce the black-body colors with residuals smaller than the differences between colors of the BB-stars and a black body spectrum. Therefore, it is not possible to discriminate if BB-stars have truly pure-He envelopes or contain a small amount of H. The actual T_{eff} of the stars will depend on their H abundance, as can be seen in the bottom panel where we show the difference between the inferred T_{BB} and T_{eff} .

5. Discussion

We find two possible scenarios that reproduce the peculiar characteristics of BB-stars. They can be explained as cool WDs with He-rich dominated with a trace of hydrogen $\log(N_{\text{H}}/N_{\text{He}}) = -5.4, -6$ and typical $\log g = 8$. This is our preferred explanation because it implies their mass is consistent with the mean mass of DBs, from which they are likely the descendants. Indeed, Koester & Kepler (2015) found that the mass distribution of DBs is strongly peaked, $\langle M_{\text{DB}} \rangle = 0.604 \pm 0.004 M_{\odot}$. The second scenario is that BB-stars are pure-He envelope massive WDs, with $\log g = 9$, roughly around $1.2 M_{\odot}$ (Althaus et al. 2005). White dwarf with these masses are expected to have an O-Ne or a CO-Ne hybrid core instead of the canonical CO core. The two scenarios we propose can be tested if distance to the

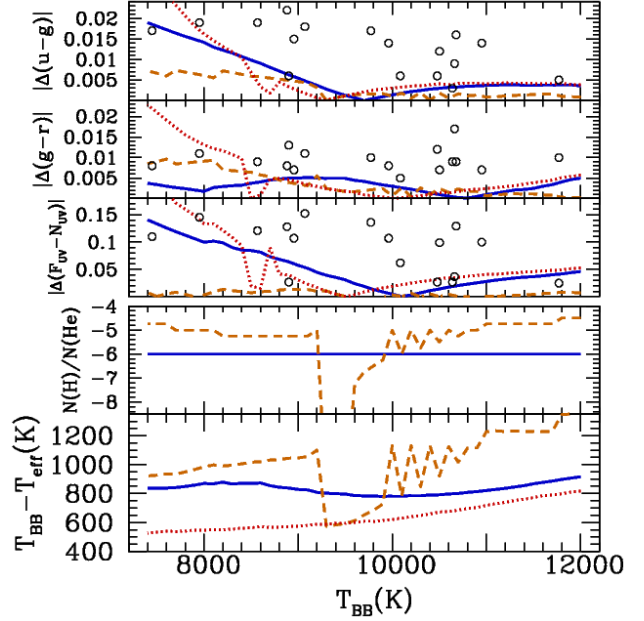


Fig. 5. Top three panels: absolute difference of colors between black-body spectrum and pure-He atmospheres (red-dotted), $\log(N_{\text{H}}/N_{\text{He}}) = -6$ models (solid blue), and best-fit model (dashed orange). Circles denote best-fit residuals for the BB-stars. Fourth panel from top: $\log(N_{\text{H}}/N_{\text{He}})$ values for the best fit model (dashed orange) and $\log(N_{\text{H}}/N_{\text{He}}) = -6$ (solid blue, constant). Lower panel: $T_{\text{BB}} - T_{\text{eff}}$ as a function of black-body temperature and hydrogen abundance for pure-He, $\log(N_{\text{H}}/N_{\text{He}}) = -6$, and best-fit models.

stars is precisely known. This will be possible with Gaia end-of-mission expectations.

Using the absolute magnitudes of the $M = 0.609 M_{\odot}$ DB evolutionary track from Althaus et al. (2009), a rough estimate of distances to the BB-stars gives 80 to 210 pc. BB-stars have g magnitudes from 17.14 to 19.44 and $(g - r)$ colors between -0.13 and 0.22 (Table 2 in SF17), which result in G magnitudes (Jordi et al. 2010) between 17.1 and 19.3. According to the Gaia end-of-mission expectations¹, parallaxes of the BB-stars will be measured with precisions between 75 and 300 μas , i.e. 1% to 6% parallax errors.

Using the relation

$$T_{\text{eff}}^4 R^2 \varpi^2 10^{0.4m_b} = cte, \quad (1)$$

the fractional uncertainty in radius R is:

$$\left(\frac{\delta R}{R}\right)^2 = \left(2 \frac{\delta T_{\text{eff}}}{T_{\text{eff}}}\right)^2 + \left(\frac{\delta \varpi}{\varpi}\right)^2 + (0.46 \delta m_b)^2, \quad (2)$$

where ϖ is the parallax and m_b the bolometric magnitude.

For a given T_{BB} , results in the bottom panel of Fig.5 show that the theoretical uncertainty in determining T_{eff} is about 5% depending on the model atmosphere that is used. In turn, T_{BB} and m_b are determined from photometry, the former to about 1-2% (SF17) and the latter to $\delta m_b \approx 0.03$, comparable to photometric errors. The dominant uncertainty is then introduced by the T_{eff} determination. Using fiducial 5% uncertainties for T_{eff} and ϖ , 0.03 for m_b , and combining quadratically the individual error sources, the precision with which R can be determined is of the order of 11%.

¹ Gaia Science Performance

The fractional radius difference between white dwarfs with $\log g = 8$ and 9, corresponding to 0.6 and 1.2 M_{\odot} respectively, is $(R_8 - R_9)/R_9 \approx \sqrt{5} - 1$, i.e. around 120% (the index refers to the $\log g$ value). This is one order of magnitude larger than the uncertainty 11% with which R could be determined, as shown above. As a result, it will be straightforward, once precise parallaxes become available, to discriminate between the normal and massive white dwarf scenario.

A follow-up question is whether or not it would be possible to test He-rich model atmospheres by determining the difference between T_{BB} and T_{eff} observationally. If the above estimation shows that the BB-stars have radii consistent with $\log g = 8$ white dwarfs, it would be reasonable to assume that their mass distribution is also typical. Koester & Kepler (2015) have found that DBs with $T_{\text{eff}} \geq 16000$ K have a strongly peaked mass distribution characterized by $\langle M_{\text{DB}} \rangle = 0.604 \pm 0.004 M_{\odot}$. Using the white dwarf models with He-rich envelopes from Camisassa et al. (2017), the radius difference between models with 0.54 and 0.66 M_{\odot} is 18%. The mass range spanned by these models is more than an order larger than the dispersion of the mass distribution of DBs. Therefore, under these hypotheses, if we assign a conservative $\delta R/R = 9\%$ to the radius, Eq. 2 can be inverted to show that T_{eff} could be determined with a 5% uncertainty. By comparing this value with the $T_{\text{BB}} - T_{\text{eff}}$ values in the bottom panel of Fig. 5, we conclude that provided that BB-stars are found to have typical DB masses, then $T_{\text{BB}} - T_{\text{eff}}$ can be determined at 1 to 2σ level for individual stars.

This is a weak measurement because it first requires using Eq. 1 to establish the nature of BB-stars by providing an estimate of their radii and then, using radii from models, to determine T_{eff} . But this procedure becomes meaningful if the nature of the BB-stars as having canonical white dwarf masses is confirmed by the Gaia measurements. If this is the case, then this assumption can be used to test if BB-stars have He-rich atmospheres with traces of H.

6. Conclusions

SF17 have discovered BB-stars that can be used as excellent calibrators for photometric surveys. Moreover, they advanced the idea that these stars could be identified as DB white dwarfs that are too cool to show any spectral signature of He. In this work, we present results of white dwarf atmosphere calculations that support this interpretation. We find that He-dominated white dwarf atmospheres in the temperature range between 12000 and 7000 K, the appropriate range in which the BB-stars have been discovered, have colors that almost exactly match those of black-body spectra.

There seems to be two scenarios that explain the characteristics of BB-stars. In one, these stars have typical WD masses around 0.6 M_{\odot} (so $\log g = 8$) and their atmospheres are He-rich with hydrogen traces around $\log(N_{\text{H}}/N_{\text{He}}) = -5.4$ or -6 . At this level, the hydrogen abundance is below the spectroscopic detection limit. In the other scenario, they are pure-He massive WDs (1 M_{\odot} or $\log g = 9$) in which the presence of hydrogen is not necessary to explain the photometric properties of BB-stars.

We consider the possibility that these two scenarios could be tested with Gaia. According to the expected end-of-mission performance, distances to the BB-stars will be determined to better than 6% and an average of 3%. Using He-pure model atmospheres, the stellar radius can be determined to about 11%, an order of magnitude smaller than the radius difference between white dwarfs with $\log g = 8$ and 9. Moreover, if the nature of the

BB-stars is that of white dwarfs with typical $\log g = 8$, consistent with the mass distribution of DBs, then their T_{eff} can be estimated to 5% level. The difference between T_{eff} and T_{BB} would then lend further support to the idea the BB-stars are cool descendants of DBs with trace abundances of hydrogen in their atmospheres.

Acknowledgements. We would like to thank Max-Planck-Institut für Astrophysik (MPA) where this work was initiated. AS is partially supported by ESP2015-66134-R and ESP2017-82674-R (MINECO). RDR thanks the support of the MINCYT (Argentina) through Grant No. PICT 2016-1128. MF thanks Hans Böhringer and Yasuo Tanaka for the hospitality at the Max-Planck-Institut für Extraterrestrische Physik and Eiichiro Komatsu at MPA, in Garching. He also thanks the Alexander von Humboldt Stiftung for support during his stay in Garching, and Monell Foundation in Princeton. He received in Tokyo a Grant-in-Aid (No. 154300000110) from the Ministry of Education. Kavli IPMU is supported by World Premier International Research Center Initiative of the Ministry of Education, Japan.

References

- Althaus, L. G., García-Berro, E., Isern, J., & Córscico, A. H. 2005, *A&A*, 441, 689
- Althaus, L. G., Panei, J. A., Miller Bertolami, M. M., et al. 2009, *ApJ*, 704, 1605
- Camisassa, M. E., Althaus, L. G., Rohrmann, R. D., et al. 2017, *ApJ*, 839, 11
- Doherty, C. L., Gil-Pons, P., Siess, L., & Lattanzio, J. C. 2017, *PASA*, 34, e056
- Fukugita, M., Ichikawa, T., Gunn, J. E., et al. 1996, *AJ*, 111, 1748
- Jordi, C., Gebran, M., Carrasco, J. M., et al. 2010, *A&A*, 523, A48
- Kepler, S. O., Pelisoli, I., Koester, D., et al. 2015, *MNRAS*, 446, 4078
- Kleinman, S. J., Kepler, S. O., Koester, D., et al. 2013, *ApJS*, 204, 5
- Koester, D. & Kepler, S. O. 2015, *A&A*, 583, A86
- Koester, D. & Knist, S. 2006, *A&A*, 454, 951
- Rohrmann, R. D., Althaus, L. G., García-Berro, E., Córscico, A. H., & Miller Bertolami, M. M. 2012, *A&A*, 546, A119
- Suzuki, N. & Fukugita, M. 2017, *ArXiv e-prints*:1711.01122
- Weidemann, V. & Koester, D. 1995, *A&A*, 297, 216